Journal of Imaging Science and Technology® 50(4): 333–340, 2006.

Nondestructive Microscopic and Spectroscopic Methods for Depth Profiling of Ink Jet Prints

Branka Lozo
Faculty of Graphic Arts, University of Zagreb, Getaldiceva 2,10000 Zagreb, Croatia
E-mail: branka.lozo@grf.hr

Jouko Vyörykkä
YKI, Institute for Surface Chemistry, P.O. Box 5607, SE-114 86 Stockholm, Sweden

Tapani Vuorinen
Laboratory of Forest Products Chemistry, Helsinki University of Technology, P.O. Box 6300, FIN-02015 HUT, Finland

Tadeja Muck
Faculty of Natural Sciences and Engineering, Department of Textiles, University of Ljubljana, Snezniska 5, 1000 Ljubljana, Slovenia

Abstract. *The binding process of printing inks on the printing substrate is one of the final phases in the creative chain of a new product formation—the print. It is not only the expected mechanism of ink drying that influences the ink distribution on the substrate surface, but also the properties of the substrate itself. Many factors, like hydrophobicity, roughness, and porosity influence the ink distribution on both coated and uncoated papers. The aim of this study was to evaluate the applicability of several nondestructive methods in the analysis of vertical and radial ink distribution on diverse ink jet prints. What are the limits and the extent of confocal Raman, ultraviolet (UV) Raman, CLSM and Fourier-transform infrared (FTIR) PAS in the analysis of ink jet ink distribution in the z direction of the print? In the experiment, both dye- and pigment-based ink jet inks were printed on different types of coated and uncoated papers. The results show a correlation between the confocal Raman and CLSM methods for depth profiling. UV Raman proved useful in the surface analysis of prints while FTIR PAS was useful for measurements at low depth in the z direction. The applied microscopic and spectroscopic methods provide a precise distinction between the upper homogeneous and the inside nonhomogeneous ink layers. Sporadic streams of deeply penetrated ink jet ink were also detected. © 2006 Society for Imaging Science and Technology.*
[DOI: 10.2352/J.ImagingSci.Technol.(2006)50:4(333)]

INTRODUCTION

Ink distribution inside a sheet is one of the parameters of print quality evaluation along with print durability, image stability, optical density, rub resistance, recyclability, and permanence properties, i.e., light and water fastness of the print. Microtome cross sections of the print may give a real insight into the ink distribution, but this method is not always applicable. The substrate may be too thick for cutting or ink may interact with the liquid media used in embedding.[1] An alternative to the cross sections of the print is the nondestructive approach to the print's inside in which the sample is typically sliced optically in the *z* direction. Various types of microscopic and spectroscopic methods found their application in studies of printing materials, such as residual lignin in the pulp,[2] paper coating analysis,[3] determination of pore volume,[4] studies of colorants,[5] offset,[6] and ink jet prints,[7,8] as well as interactions during printing.[9]

The aim of this study was to observe the behavior of a wide choice of papers printed with both dye- and pigment-based ink jet inks. The use of ink jet coated photopaper as a printing substrate together with other nonspecialized coated and uncoated papers enables the comparison of ink migration inside the sheet. Nondestructive spectroscopic measurements provide the depth profiling of each ink-substrate combination. Depth profiling represents a tool for print quality evaluation and troubleshooting. This is based on information coming not only from the print surface, but also from beneath it.

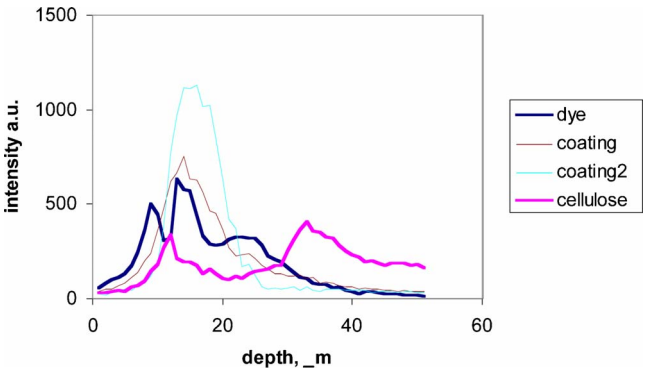

Figure 1. Representative Raman depth profile of dye-based print on photopaper.

Received Aug. 11, 2005; accepted for publication Dec. 13, 2005.
1062-3701/2006/50(4)/333/8/$20.00.

Furthermore, we wanted to get detailed insight into the ink distribution in the *z* direction of the prints as well as to make a distinction between the upper (homogeneous) and lower (nonhomogeneous) ink layers.

Another objective of this study was to evaluate the extent and limit of each method used for the measurements of vertical ink penetration and radial ink distribution.

MATERIALS AND METHODS

Materials

Materials used in the experiment were as follows:

Z—Zweckform photopaper, recommended for ink jet prints, one-side coated, high gloss (130 g/m^2, 170 μm);

K—Carton board, one-side coated multilayered white board (300 g/m^2, 430 μm);

I—ICP permanent paper made at the Pulp and Paper Institute in Ljubljana, which corresponds to standard ISO 9706, no surface treatment (70 g/m^2, 110 μm);

T—Three-ply tissue paper with a low percentage of secondary fibers (60 g/m^2, 185 μm).

Prints were done on the Canon BJC 8500 ink jet printer with dye-based ink and the Epson Stylus photo 2100 printer with pigment-based inks. Printing quality was 1200 dpi with color intensity 100%.

Raman Microscopy

The confocal Raman spectra were collected with a dispersive Kaiser Optical Systems Hololab Series 5000 Raman microscope. The exiting laser operated at 785 nm and the maximum laser power at the sample stage was 85 mW. The laser power was decreased to 74 mW in order to achieve better quality Raman spectra of ink jet inks. Oil immersion objective (100×, numerical aperture 1.30) was used with the immersion sampling method, which is described in detail elsewhere.[10] The depth resolution was determined by analyzing the derivative of thick polymer film depth profile.[11] The analyzed depth resolution was 3.5 μm and the lateral resolution was approximately 2 μm. A set of measurements was performed with a 20 μm lateral movement in the *x* direction to increase the spot size in the *x* direction while maintaining the depth resolution. The distance between two parallel measurements was 34.4 μm. Collected Raman spectra were processed by a MATLAB program, which extracts the peak heights from the Raman spectra. It was possible to identify six Raman peaks from the spectra, which were then converted to the depth profiles.

Confocal Laser Scanning Microscopy

The Zeiss Axiovert 100M confocal scanning microscope was used. The numerical aperture of the objective was 0.6 and the laser wavelength was 458 nm. The emission was observed through green, 530 nm, and red, 560 nm, filters. The scan area was 200 μm × 200 μm and resolution in the *z* direction was 2.7 μm. The sample was virtually sliced in the *z* direction by a scanner in intervals varying between 0.73 and 0.81 μm. The data were processed by the Zeis LSM image browser program.

Sample preparation

For CLSM the samples were also prepared with immersion oil. It partly increases the transparency of the sample enabling the re-emission from deeper levels. Sigma inert mineral oil was used for both sides of samples. The cover glass was fixed on the sample.

Fourier Transform Infrared Photoacoustic Spectroscopy

The Bio Rad 6000 infrared spectrometer was used with UMA 500 microscope. The measurements were done in midinfrared region. The collected spectra were processed by DIGILAB WIN IR PRO program.

Sample preparation

All the samples were dried before the measurements, since paper humidity introduces noise in the spectra. Samples were dried 4 h at 60 °C and then placed in the measurement chamber of the photoacoustic unit.

Ultraviolet Raman Spectroscopy

The Renishaw 1000 ultraviolet (UV) Raman microscope was equipped with Leica microscope and Innova 90 FreD frequency doubled Ar^+ ion laser (Coherent, Inc., CA) providing continuous wave laser light in the UV region (between 229.0 and 264.3 nm). The laser wavelength used in this work was 244 nm and the laser power at the sample stage was approximately 2 mW. UV Raman spectra were collected with a deep UV LMU-15× objective (OFR Inc.).

Sample preparation

For UV Raman spectroscopy the samples were fixed on glass slides and no further preparation was needed. During the measurements the samples were spinned at a speed of 6 rpm (i.e., 1,5 mm/s) in order to avoid sample burning.

RESULTS AND DISCUSSION

Raman Depth Profiles

Photopaper

Depth profiles obtained from the Raman spectra of printed photopaper (*Z* sample) were analyzed. The results in Table I are the mean values of 14 measurements for dye-based ink and of 16 measurements for pigment-based ink. Ink layers were classified according to the intensity into three categories: compact, noncompact, and deep. The grades differ for dye-based and pigment-based inks due to differences in the maximum intensity value. For the pigment-based ink the maximum intensity approached 12 000 while for the dye-based ink it barely reached 1700 indicating that pigment based inks induce much stronger Raman scattering. The compact ink layer was typically the most intense part of the ink curve. If the curve had two peaks, it was always the first one that was considered as the compact layer. In the case of a more intense second peak the ink layer presented nonhomogeneity of ink distribution and was therefore classified as a noncompact layer (Fig. 1). The results classified as *deep* were interpreted as representing maximum ink penetration. For all measured samples these exhibited at the same time minimum scattering intensity.

Table I. Raman depth profile analysis of the *Z* sample.

Z sample	Thickness of ink layers					
Type of *IJ* ink	Dye based			Pigment based		
Ink layer categories	Compact	Noncompact	Deep	Compact	Noncompact	Deep
Intensity (a.u.)	>300	200–300	<200	>1000	500–1000	<500
Ink thickness (μm)	3.1	10.4	14.8	4.8	8.6	13.5
Interval (μm)	0–8	0–17	0–32	3–9	5,5–12	7–26

The compact ink layer of pigment-based ink was about 5 μm thick with a major part of the ink remaining on the paper surface. A smaller amount of the compact ink layer was observed to penetrate into the paper coating. The compact layer was followed by the noncompact ink layer as in the case of dye-based inks. Typically (in 13 of 16 cases), the curve declined gradually as the ink intensity diminished. In three cases the curve formed another ink pigment peak beneath the paper coating (Fig. 2). The gap between the two ink layers was 8 μm and the analyzed thickness of the second ink layer was 7.5 μm. The average ink penetration was 13.5 μm and the highest measured value for ink penetration was 26 μm (Table I). The thickness of the paper coating layer was approximately 12.5 μm.

The analyzed thickness of the compact ink layer of the dye-based ink was about 3 μm. In five of 14 cases the dominant intensity of the compact layer was detected on the coating surface; in six cases the compact layer was located inside the paper coating nearest to the surface; in three cases there was almost no ink registered. The noncompact ink layer formed the second ink peak in seven cases, in five of which the second peak was more intense than the first one. The maximum ink penetration depth was generally deeper for the dye based than for the pigment-based ink, expressed as mean value (14.8 μm) as well as highest measured value (32 μm). In four cases the ink penetrated through the paper coating layer and reached the cellulose in the base paper.

Analysis of the depth profiles showed mobility of dye-based ink in both radial and vertical distribution.

The surface of the *Z* sample is not homogeneous. Narrow cracks on the coating layer are made on purpose to improve the ink penetration. Through the cracks ink reaches the depths that would otherwise be unattainable through the coating layer. Once under the coating, ink spreads in radial as well as in vertical direction. This explains the presence of second ink peak in the depth profile curve.

Some cracks are too narrow for the pigmented ink to penetrate. Pigments (ca. 0.8 μm) typically concentrate at the edges of such cracks which yield an extremely intense signal in depth profile (Fig. 3). On the contrary, dye-based inks will be sucked by strong capillary forces into the crack showing almost no signal in the depth profile (Fig. 4).

Carton board, ICP permanent paper, tissue paper

Collecting the Raman spectra from *K*, *I*, and *T* samples was very difficult, partially because the uncoated sample surfaces were very inhomogeneous, containing large pores and, hence, leading to inhomogeneous ink distribution on the surface on the confocal Raman scale (2 μm). Moreover, a laser burned the inks if a high laser power was used. From a series of mostly unsuccessful measurements it was possible

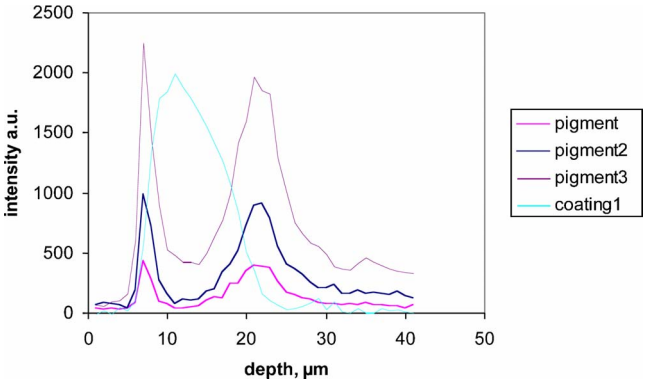

Figure 2. Representative Raman depth profile of pigment-based print on photopaper.

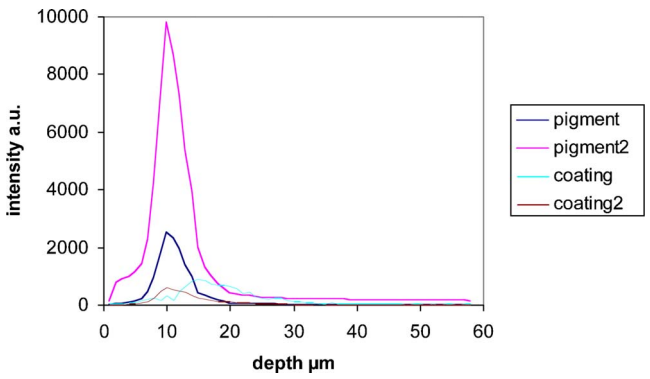

Figure 3. Typical Raman depth profile of pigment-based print on photopaper.

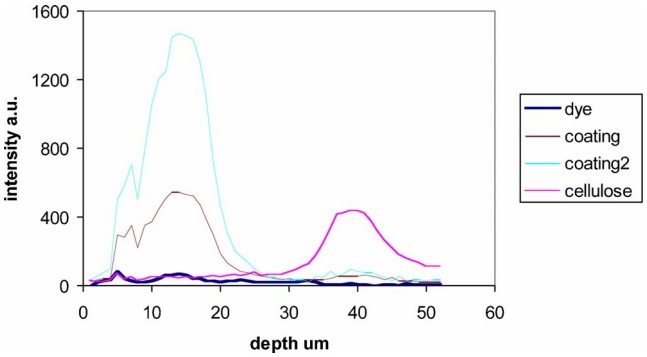

Figure 4. Representative Raman depth profile of dye-based print on photopaper.

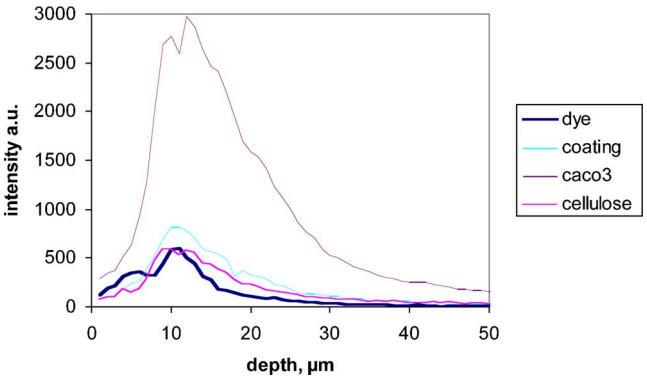

Figure 5. Representative Raman depth profile of dye-based print on carton board.

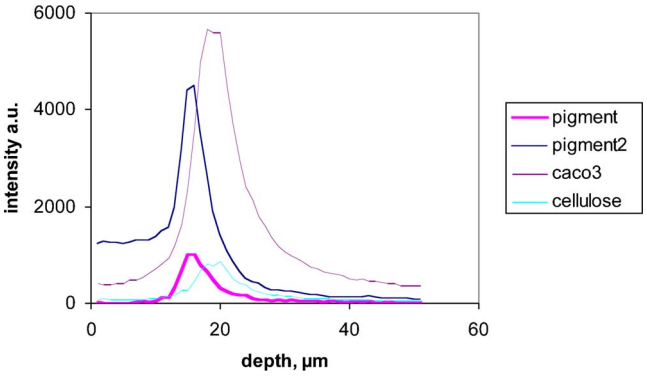

Figure 6. Raman depth profile of pigment-based print on carton board.

to separate several successful spectra of *K* and *I* samples, but the number of measurements were not sufficient for statistical analysis (see Figs. 5–8).

Confocal Laser Scanning Microscopy

CLSM enables us to see the picture of each of the virtual slices in the *z* direction of the print. It also gives the orthogonal projection of the marked *x* and *y* line in the picture (Fig. 9). The elaboration of the orthogonal projection includes the following steps: measuring the number of virtual slices according to the ink penetration; classifying the results

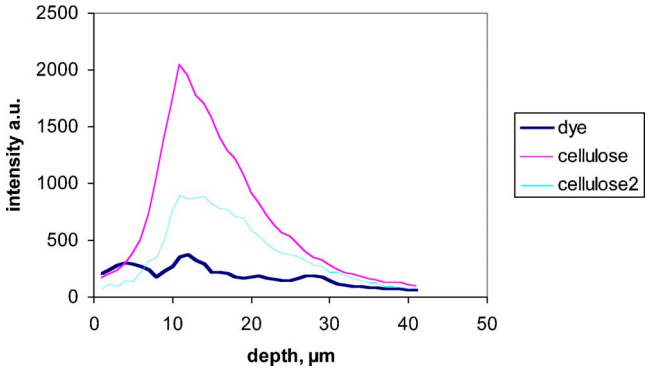

Figure 7. Raman depth profile of dye-based print on ICP permanent paper.

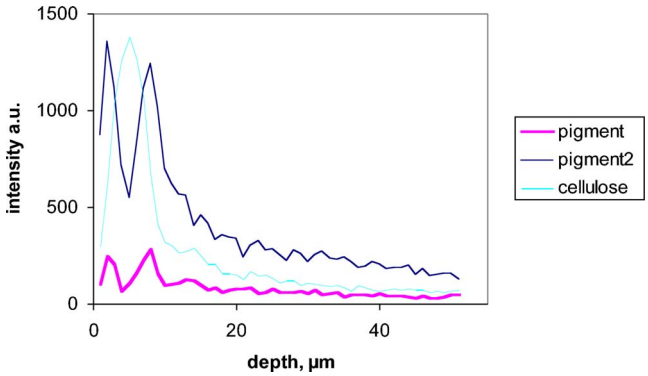

Figure 8. Raman depth profile of pigment-based print on ICP permanent paper.

in three grades as homogeneous ink layer, nonhomogeneous ink layer, and the maximum ink penetration; converting the measured number of slices into the depth of penetrated ink expressed in micrometers. The thickness of virtual slices vary from 0.73 to 0.81 μm. All samples were successfully measured and processed. Elaborated results are presented in Table II.

In the interpretation of CLSM results the homogeneous ink layer corresponds to the compact ink layer from the Raman depth profiles. The nonhomogeneous ink layer corresponds to the noncompact ink layer and the maximum of ink penetration corresponds to the deepest ink penetration.

Photopaper

It is obvious that the CLSM results are not congruous with figures of the Raman depth profiles, but they correlate with respect to the three categories. The homogeneous ink layer of dye-based ink is thinner than the pigment-based ink (1.95 μm $\neq$ 2.50 μm).

Dye-based ink penetrates deeper than pigment-based ink in nonhomogeneous ink layer (14.67 μm $\neq$ 9.00 μm). The maximum ink penetration was also greater for the dye-based ink than for the pigment-based ink (23.53 μm $\neq$ 20.92 μm).

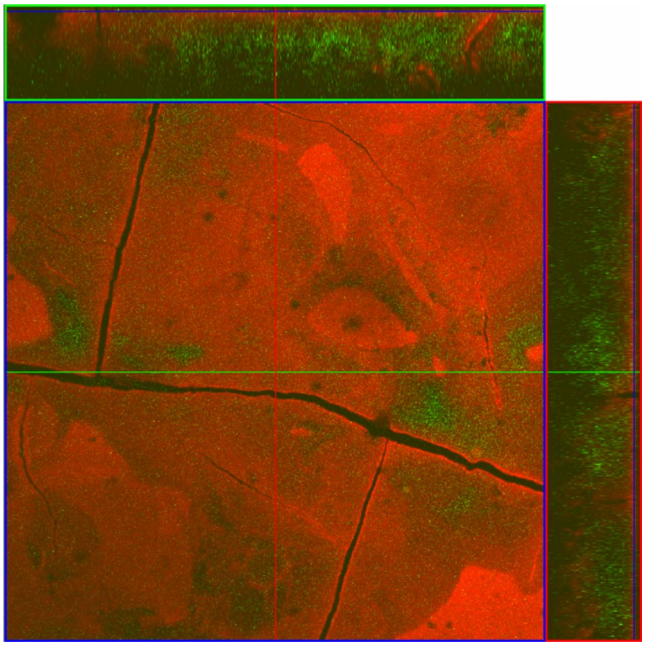

Figure 9. CLSM picture of dye-based print on photopaper.

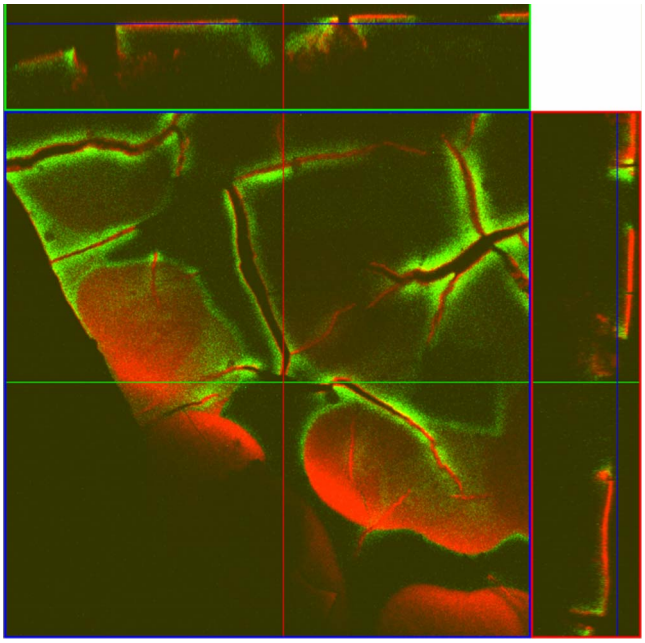

Figure 10. CLSM picture of pigment-based print on photopaper.

The same model of ink behavior was seen in the Raman depth profiles: the compact layer of pigment-based ink was thicker while the dye-based ink penetrated deeper with lower intensity.

CLSM pictures of the surface of the prints show the microcracks in the paper coating structure (Figs. 9 and 10).

Cracks are visible in detail. We can see the ink pigments concentrated at the edges of the cracks forming "rivers" or "capillaries" all over the measured area. Very high intensity of ink pigment signals, over 10 000, in confocal Raman depth profile originated from "river" edges and capillaries. The behavior of the dye-based ink is different: ink is sucked into the cracks, no capillaries are visible. When confocal Raman measurement took place precisely above the crack, the depth profile showed only minor signal or no signal at all from the dye.

Besides the analysis of the surface structure of the print and distribution of the penetrated ink, CLSM measurements enables the analyses of the orthogonal structure of the cracks. From the orthogonal projection the diameter of the crack was measured: it varied from 0.8 to 5.6 μm dividing the coating surface in asymmetrical areas. Through the cracks the sporadic streams of deeply penetrated ink are created.

Carton board, ICP permanent paper, tissue paper

Pigment-based ink remained in a thin homogeneous layer on the coating surface (3.58 μm when printed on sample *K*). The nonhomogeneous layer was thick (6.50 μm) and hardly visible. Dye-based ink penetrated deeply into the coating forming a thicker homogeneous layer (6.67 μm). The nonhomogeneous layer is also thicker (13.81 μm). The maximum of ink penetration is presented sporadically in both of the *K* prints (dye and pigment based).

Sample *I* is uncoated paper, so the ink comes into direct contact with the cellulose fibers. The measurement of the homogeneous ink layer is in fact the measurement of ink deposited onto the surface of the upper cellulose fibers in the paper structure.

The pigment-based ink formed a bit thicker homogeneous layer than the dye-based ink (3.04 μm $\neq$ 2.13 μm). The other two ink layers, the nonhomogeneous and the maximum of ink penetration, were determined by the paper structure: the cellulose fibers lead into the paper inside. In Fig. 11 the fiber structure and cavities between them are visible.

Sample *T* is also uncoated paper and therefore ink and cellulose fibers are in direct contact, too. Sample *T* differs from sample *I* in surface roughness and structure porosity. This allows good ink mobility inside the sheet, particularly in the vertical direction. The measured maximum ink penetration depth was 39.50 μm for the pigment-based ink and 49.95 μm for the dye-based ink. This was the deepest ink penetration depth measured in our study.

Fourier Transform IR Photoacoustic Spectroscopy

From the spectra collected by Fourier-transform infrared (FTIR) PAS measurements it is obvious that the signal is obtained from at least 5 μm beneath the print surface. To be certain of this conclusion the unprinted *Z*, *K*, *I*, and *T* samples were measured. In Figs. 12, 13, 14, and 15 the spectra are presented in groups according to the base paper.

The concordance within each group of signals was almost complete. A disharmony appeared only in the intensity of the *Z* and *K* group of samples and slightly in the *T* group. The results of Raman depth profiles and CLSM orthogonal projections showed that the thickest compact ink layer was on the *Z* sample printed with the pigment-based ink. Com-

Table II. CLSM orthogonal projection analysis.

	Thickness of ink layers (μm)					
	Dye-based ink			Pigment-based ink		
Samples	Homog.	Nonhomog.	Max.	Homog.	Nonhomog.	Max.
Z	1.95	14.67	23.53	2.5	9.0	20.92
K	6.67	13.81	18.99	3.58	6.5	10.38
I	2.13	10.82	19.2	3.04	9.48	13.96
T	4.59	9.99	49.96	3.96	9.48	39.5

pact and homogeneous ink layers in all other samples were thinner. The thickness of the paper coating layer of the *Z* sample was 12.5 μm. The concordance of the FTIR PAS spectra from the unprinted *Z* sample, the dye-based printed *Z* sample, and the pigment-based printed *Z* sample proves that the signal was collected from the depth interval of approximately 5–10 μm. The concordance of the spectra also showed that the intensity of noncompact or nonhomogeneous ink layer was low, because there was no dye or pigment peak registrated in the spectra.

The same model of very similar spectra within each of group of *K*, *I*, and *T* samples is shown in Figs. 13, 14, and 15.

UV Raman Spectroscopy

It was possible to get resonance enhanced UV Raman [UV Resonance Raman (UVRR)] spectra as the inks used in this work had conjugated double bonds absorbing the exciting laser light. The criteria for the concordance within the UVRR spectra of the measured samples are the types of ink jet ink (Figs. 16 and 17).

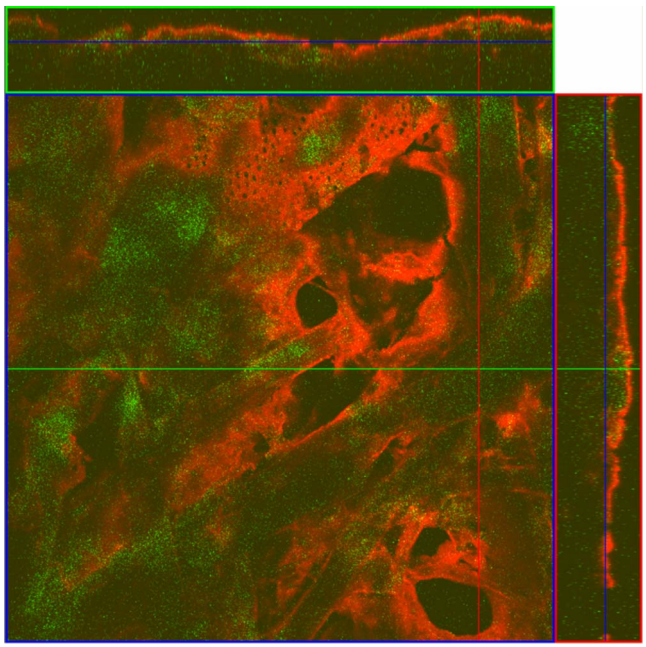

Figure 11. CLSM picture of dye-based print of ICP paper.

The concordance of the spectra within the dye-based and pigment-based prints, irrespective of the printing substrate, means that the signal was collected from the very surface of the sample. In UVRR microscopy the analysis depth is limited by the absorbance of the ink, which may typically be around 1 μm.

Disproportion in intensity which was small for pigment-based prints and more evident for dye-based prints, can be explained by the CLSM result (Table II). It was obvious that the intensity of UVRR spectra correlated with the thickness of the homogeneous ink layer: the most intensive signal for the *Kd* sample came from a 6.67 μm thick ink layer; it was followed by the *Td* sample from a 4.59 μm thick ink layer; *Zd* and *Id* signals were similar, of low intensity since their homogeneous ink layers were thin (1.95 and 2.13 μm, respectively).

The same analogy was applicable for pigment-based prints, although the differences in the intensity of the UVRR spectra were less pronounced.

CONCLUSIONS

The Raman depth profiles showed a detailed structure of print components marked out on the Raman spectra. The advantage of direct depth profiling by the confocal Raman method is that it delivers information of chemical components and their distribution without the need of labeling or other pretreatment. Along with the analysis of dye and pigment components, we could analyze the paper structure: coating and cellulose distribution in the *z* direction. It was observed that the intense laser power can easily burn the surface of uncoated and conventionally coated papers as well as inks. Pigment-based ink jet ink formed a thicker compact layer on the paper surface, while dye-based ink penetrated deeper.

The CLSM orthogonal projections enabled an insight into the virtually cut area. Since the measured area was ca. 200 × 200 μm, the ink migration inside the sheet could be realistically represented. Those projections confirmed the Raman depth profile analysis of the *Z* samples: the ink for-

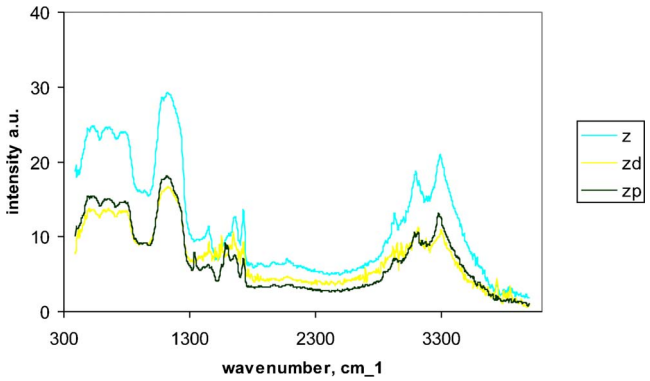

Figure 12. FTIR PAS spectra of *Z* samples.

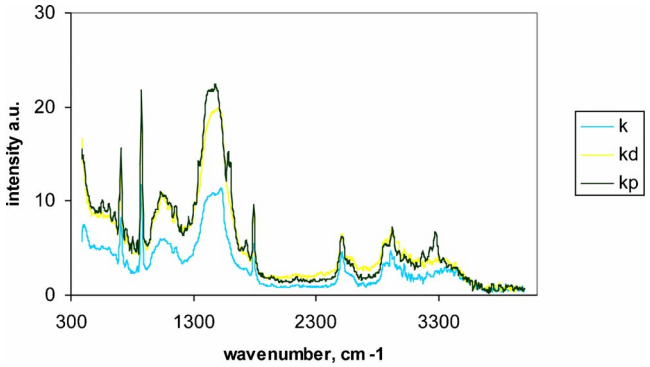

Figure 13. FTIR PAS spectra of *K* samples.

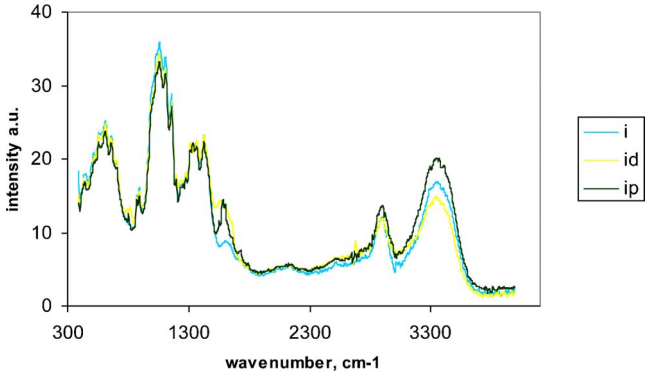

Figure 14. FTIR PAS spectra of *I* samples.

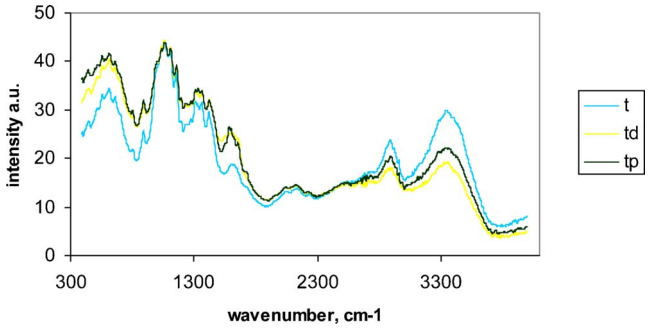

Figure 15. FTIR PAS spectra of *T* samples.

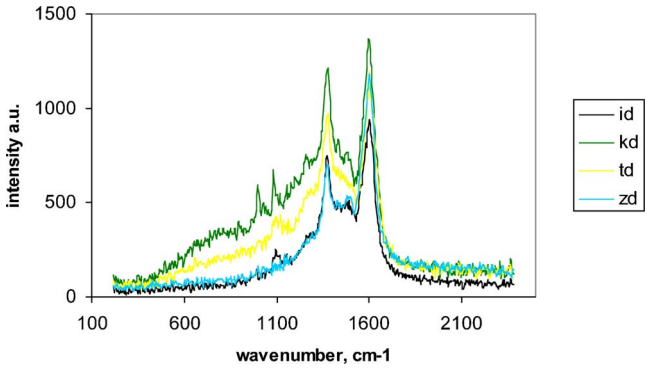

Figure 16. UVRR spectra of dye-based prints.

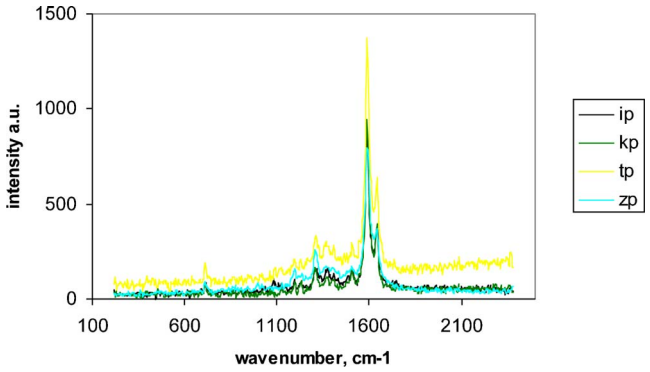

Figure 17. UVRR spectra of pigment-based prints.

mation in levels of intensity—thicker for pigment-based ink, deeper for dye-based ink. The CLSM orthogonal projection makes it possible to study the paper structure: the distribution of cracks on the photopaper surface as well as their diameter and depth; individual fibers and interfiber cavities in uncoated samples. These structures can be registered due to the ink distribution on and beneath the printed surface. If the ink did not penetrate throughout the coating layer to the base paper cellulose, it was not possible to define the thickness of the coating layer, either for *Z* or *K* samples.

The FTIR PAS spectra are collected from the depth of 5–10 μm beneath the surface ink layer. For coated papers it was the coating layer which was analyzed by the FTIR PAS method. For coated papers it is the coating layer which is analyzed. The quantity of ink at the depth involved in FTIR PAS measurements was negligible.

The UVRR spectra are collected from the very surface of the printed area. UVRR spectra correlated well with the type of ink, irrespective of the differences in printing substrates. The relation with the thickness of the surface ink layer was possible to observe from the intensity of the spectra: the thicker the ink layer, the more intense the spectrum.

Despite the limits of each of the applied nondestructive methods, the diversity of their possibilities enables a precise insight into the interior of the print.

ACKNOWLEDGMENTS

The authors would like to thank Mrs. Rita Hatakka, HUT, for her great help with Raman, UV Raman, and FTIR measurements. The Croatian Ministry of Science, Education and Sport partly supported the research with Grant No. 533-06-05-2.

REFERENCES

[1] T. Muck, B. Lozo, L. Otahalova, M. Drzkova, and M. Kaplanova, "Non-destructive methods in the study of IJ ink-substrate interaction", *Proc. IARIGAI 2005*, Porvoo, Finland, pp. 239–247.

[2] A.-M. Saariaho, B. Hortling, A.-S. Jääskeläinen, T. Tamminen, and T. Vuorinen, "Simultaneous quantification of residual lignin and hexenuronic acid from chemical pulps with UV resonance Raman spectroscopy and multivariate calibration", J. Pulp Pap. Sci. **29**, 363 (2003).

[3] J. Vyörykkä, K. Juvonen, D. Bousfield, and T. Vuorinen, "Raman microscopy in lateral mapping of chemical and physical composition of paper coating", Tappi J. **3**, 19 (2004).

[4] K. Vikman, "Fastness properties of ink jet prints on coated papers—Part 1: Effect of coating polymer system on light fastness", J. Imaging Sci. Technol. **47**, 30 (2003).

[5] M. Kaplanová, "Photoacoustic study of the optical and thermal properties of printed samples", J. Prepr. Print. Tech **2**, 4 (1998).

[6] J. Vyörykkä and T. Vuorinen, "Confocal Raman microscopy: A nondestructive method to analyse depth profiles of coated and printed papers", Nord. Pulp Pap. Res. J. **19**, 218 (2004).

[7] K. Vikman, "Fastness properties of ink jet prints on coated papers—Part 2: Effect of coating polymer system on water fastness", J. Imaging Sci. Technol. **47**, 38 (2003).

[8] K. Vikman and T. Vuorinen, "Water fastness of ink jet prints on modified conventional coatings", J. Imaging Sci. Technol. **48**, 138 (2004).

[9] K. Vikman and K. Sipi, "Applicability of FTIR and Raman spectroscopic methods to the study of paper-ink interactions in digital prints", J. Imaging Sci. Technol. **47**, 139 (2003).

[10] J. Vyörykkä, M. Halttunen, H. Iitti, J. Tenhunen, T. Vuorinen, and P. Stenius, "Characteristics of immersion sampling technique in confocal Raman depth profiling", Appl. Spectrosc. **56**, 776 (2002).

[11] J. Vyörykkä, J. Paaso, M. Tenhunen, J. Tenhunen, H. Iitti, T. Vuorinen, and P. Stenius, "Analysis of depth profiling data obtained by confocal Raman microspectroscopy", Appl. Spectrosc. **57**, 1123 (2003).